Preparation and Characterization of the Solid Solution Series $Co_{1-x}Ni_xAsS$ $(0 \leqslant x \leqslant 1)$*

J. J. STEGER, H. NAHIGIAN, R. J. ARNOTT, AND A. WOLD

Department of Chemistry and Division of Engineering, Brown University, Providence, Rhode Island 02912

Both single crystal and polycrystalline samples of the series $Co_{1-x}Ni_xAsS$ $0 \leqslant x \leqslant 1$ have been prepared. The materials have been characterized by X-ray diffraction, density, and chemical analysis. X-ray intensity data collected for the end member NiAsS shows anion ordering consistent with the ullmanite structure (space group $P2_13$). Magnetic data indicate that nickel (d^7) is present in the low-spin state. Electrical data show that one additional electron/Ni atom is contributed to the otherwise empty σ^* band of CoAsS.

Introduction

The combination of simple structure types and diverse magnetic and transport properties has led to numerous investigations (*1–9*) of transition metal chalcogenides and pnictides. In particular, materials which crystallize in the cubic pyrite structure exhibit properties ranging from metallic ferromagnetism (e.g., CoS_2 (*6*)) to diamagnetic semiconducting (e.g., FeS_2-*p* (*7*)). These variations in properties have been attributed to the occupancy and degree of correlation of electrons in an isolated σ^* band ((*8*) Fig. 1).

CoAsS has been reported (*9*) to be a diamagnetic semiconductor where Co^{3+} (low-spin d^6) is present in an octahedral field. CoAsS was found (*9*) to crystallize with the cubic pyrite structure when prepared at temperatures above 800°C. NiAsS (the mineral gerrsdorffite) has been reported (*10*) to have the cubic ullmanite structure (Fig. 2) ($a = 5.68$ Å and space group $P2_13$). Preparation of the solid solution series $Co_{1-x}Ni_xAsS$ $(0 \leqslant x \leqslant 1)$ by direct combination of the elements has been reported by Klemm (*11*).

He reported cubic unit cell parameters that ranged from 5.572 Å for CoAsS to 5.693 Å for NiAsS.
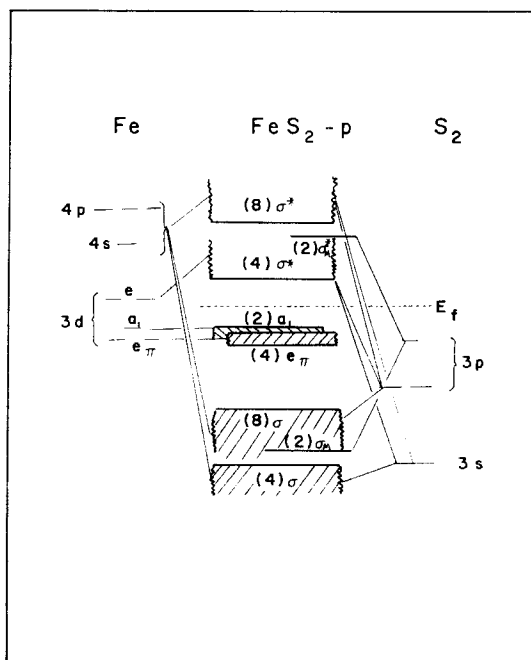
FIG. 1. One-electron energy level scheme for FeS_2.

53
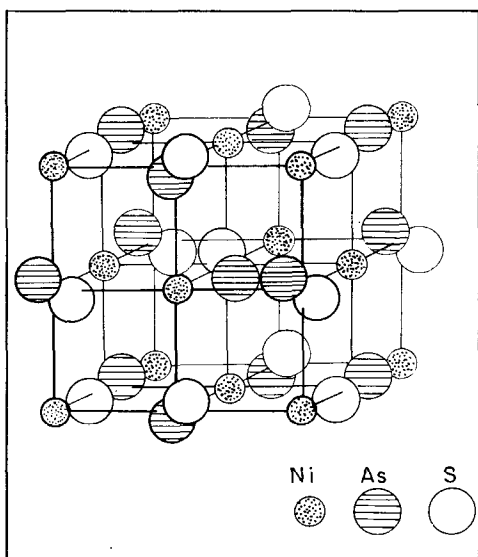
Ni   As   S

FIG. 2. Anion-ordered NiAsS-cubic ullmanite structure.

Substitution of As for S in CoS_2 (Co^{2+} d^7 low-spin (4)) results in a depopulation of electrons from the σ^* antibonding band (8) and a subsequent dilution of ferromagnetic interactions across the series $CoAs_xS_{2-x}$ $0 \leqslant x \leqslant 1$. The possibility of repopulating the σ^* band by a progressive substitution of nickel (d^7) for cobalt (d^6) has prompted this study of the series $Co_{1-x}Ni_xAsS$ ($0 \leqslant x \leqslant 1$).

Preparation

Polycrystalline samples of the series $Co_{1-x}Ni_xAsS$ ($0 \leqslant x \leqslant 1$) were prepared by direct combination of the elements. Single crystal samples for $0 \leqslant x \leqslant 0.4$ were grown by chemical vapor transport. Pretreatment of the starting materials was as follows: The high-purity metals (Co 5–9's and Ni 5–9's)[1] were reduced (Co at 850°C for 8 hr and Ni at 600°C for 3 hr) in a 15% H_2/85% Ar atmosphere. High purity arsenic (As 6–9's) was sublimed for 3 hr at 200°C under dynamic vacuum to remove volatile components. Elemental sulfur (6–9's) was used as supplied.

Stoichiometric quantities of the elements were placed into silica tubes and evacuated for approximately 4 hr to a pressure below 2 μm. The transport tubes were then backfilled to 50–100 Torr with Cl_2 gas (Matheson Co., East Rutherford, N.J.) after which all tubes were sealed off for reaction.

Preparation of single crystals by chemical vapor transport was carried out in a variable zone furnace. The furnace conditions generally ranged from 875°C in the charge zone to 625°C in the growth zone and were maintained at these temperatures for 10–14 days.

The polycrystalline samples were reacted in a large muffle furnace with the samples positioned in the furnace so as to minimize the temperature gradient across the tubes. Temperature gradients > 5°C favor incomplete reaction of the sample with the appearance of As_2S_3. For the initial reaction the temperature was raised to 800°C over a period of two days. Samples were held at this temperature for a period of eight days and then were cooled slowly (two days) to room temperature. The samples were ground in a dry nitrogen atmosphere, resealed in evacuated silica tubes, and rereacted under the same conditions. A second grinding and third reaction period were employed to insure homogeneity and reaction completeness.

X-Ray Characterization

Powder diffraction tracings for all samples were obtained with a Norelco diffractometer using monochromated radiation from a high intensity Cu source ($\lambda K\alpha_1 = 1.5405$ Å). Cell parameters were determined by a least squares refinement of the high angle reflections ($80° < 2\theta < 140°$) relative to a silicon standard.

Room temperature (296°K) intensity data for NiAsS samples were collected by accumulating counts while scanning (1/4°/min) over each reflection. The background values were subtracted from the total intensity values for each peak. Refinement of variable atomic-position parameters, occupancy factors, and unit cell temperature factor was accomplished using a Fortran program which minimized the discrepancy factor

$$R = 100(\sum |I_{cal} - I_{obs}|/\sum I_{obs}).$$

The atomic scattering factors for Ni^{3+}, As^0, and S^0 were those of Cromer and Waber (*12*) while the real and imaginary part of the anomalous dispersion factor were taken from Cromer (*13*). The intensity data were corrected for the polarization due to the curved graphite diffracted-beam monochromator.

Density Measurements

Densities of the samples were measured using a hydrostatic technique (*14*). The density fluid was perfluoro(1-methyldecalin) (Pierce Chemical Co., Rockford, Ill.), and all densities are reported with respect to the density of a single crystal silicon standard ($\rho = 2.328$ g/cm^3). The results of these measurements are given in Table I along with other physical data.

Nickel Analysis

Samples were analyzed for nickel content by the dimethyl glyoxime method (*15, 16*). The samples were dissolved by refluxing in a 6 N HCl solution to which several drops of Br_2

had been added. The results of the analyses are given in Table I.

Magnetic Measurements

Magnetic susceptibility data were obtained using a Faraday balance (*17*) equipped with a Cahn RG Electrobalance, over the temperature range 77–298°K. Measurements were performed at field strengths between 6.25 and 10.30 kOe. The balance was calibrated using the cobalt complex ($HgCo(CNS)_4$ with $\chi_g = 16.44 \cdot 10^{-6}$ cgs/g) as a standard (*18*) and temperatures were measured with a platinum resistance thermometer. Diamagnetic corrections ($Co^{3+} - 10$, $Ni^{2+} - 12$, $As^{3+} - 9$, $S^{-2} - 38 \cdot 10^{-6}$ (*19*)) were applied to the paramagnetic susceptibility data. The pertinent magnetic parameters were determined by a linear least squares analysis of the corrected paramagnetic data. Characteristic plots of the corrected inverse susceptibility as a function of temperature are shown in Figs. 3a and 3b. The values of the various magnetic parameters for the compositions studied are summarized in Table II.

TABLE I

DENSITY AND ANALYSIS FOR THE $Co_{1-x}Ni_xAsS$ COMPOUNDS

$Co_{1-x}Ni_xAsS$	ρ_{calc}(g/cm^3)	ρ_{obs}(g/cm^3)	% Ni_{calc}	% Ni_{obs}
Polycrystalline samples				
$x = 0.0$	6.36	6.36(2)	0	0
0.05	6.34		1.77	
0.1	6.31		3.54	3.5(2)
0.2	6.27	6.29(3)	7.08	
0.3	6.23		10.62	10.9(2)
0.4	6.19		14.16	
0.5	6.15	6.15(3)	17.70	17.6(3)
0.6	6.12		21.25	21.3(2)
0.7	6.08	6.07(2)	24.79	24.5(2)
0.8	6.05		28.34	
0.9	6.01		31.89	32.3(3)
1.0	5.99	5.99(3)	35.43	
Single crystal samples				
$x = 0.0$	6.36	6.35(1)	0	0
0.05	6.34	6.32(2)	1.77	1.8(2)
0.1	6.31	6.31(1)	3.54	3.6(2)
0.2	6.27	6.27(3)	7.08	7.1(3)
0.3	6.23	6.24(4)	10.62	10.0(5)
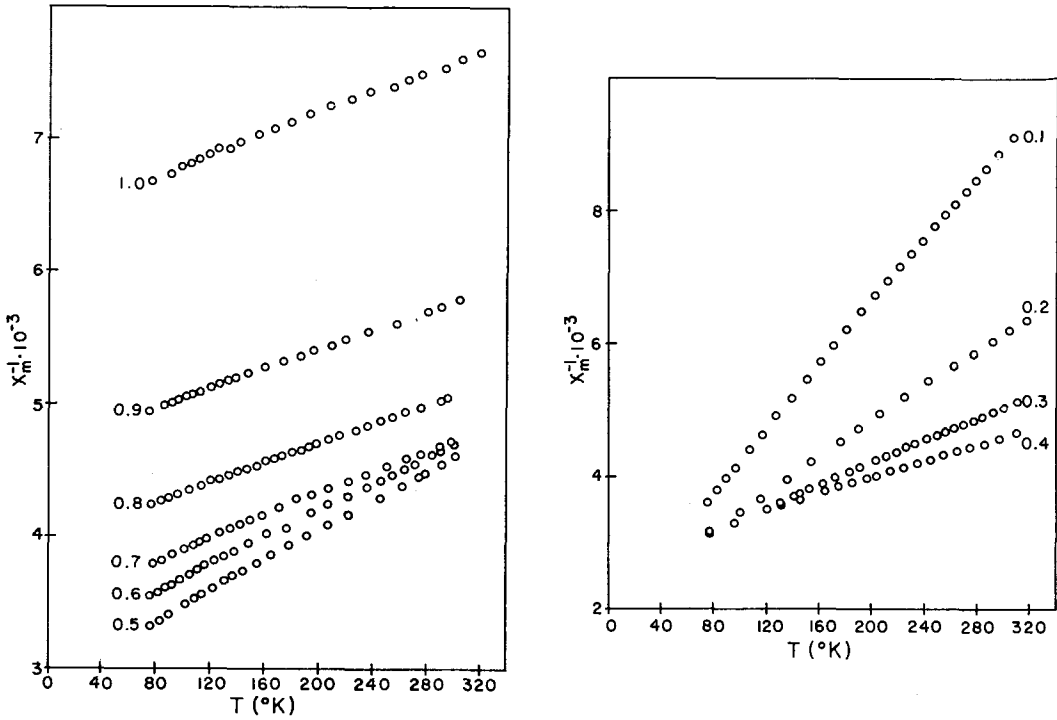
FIGS. 3a (left) and 3b. (right) Inverse susceptibility χ_M^{-1} vs temperature (°K) for the $Co_{1-x}Ni_xAsS$ compounds.

Electrical Measurements

Resistivity and Hall effect measurements were made over the temperature range (77–340°K). Crystals were lapped to a uniform thickness after which indium leads were attached using an ultrasonic soldering technique. The irregularly shaped crystal perimeter required use of the van der Pauw method (20).
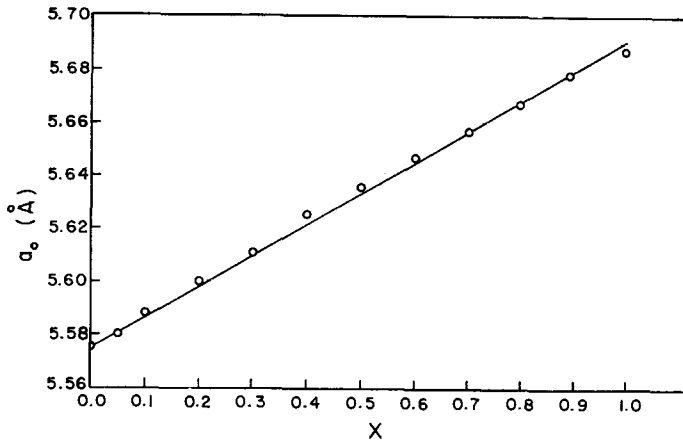
FIG. 4. Cell constants a_0 vs composition x for $Co_{1-x}Ni_xAsS$ ($0 \leqslant x \leqslant 1$).

TABLE II

PARAMAGNETIC MOMENTS, WEISS CONSTANTS AND
LATTICE PARAMETERS FOR THE $Co_{1-x}Ni_xAsS$
COMPOUNDS

$Co_{1-x}Ni_xAsS$	$P_{eff}/Ni(\mu_B)$	$\theta_p(°K)$	$a_0(Å)$
Polycrystalline samples			
$x = 0.0$			5.576(2)
0.05	1.74(1)	−45(2)	5.580(3)
0.1	1.79(1)	−80(4)	5.591(3)
0.2	1.67(3)	−143(10)	5.601(3)
0.3	1.73(2)	−272(9)	5.612(3)
0.4	1.73(2)	−396(13)	5.625(3)
0.5	1.71(2)	−539(17)	5.635(3)
0.6	1.63(2)	−633(14)	5.646(3)
0.7	1.66(2)	−848(25)	5.656(4)
0.8	1.68(1)	−1120(16)	5.666(3)
0.9	1.69(2)	−1367(29)	5.679(3)
1.0			5.685(2)
Single crystal samples			
0.0			5.576(2)
0.05	1.80(2)	−43(1)	5.580(2)
0.1	1.81(4)	−84(1)	5.588(2)
0.2	1.70(5)	−132(2)	5.600(2)
0.3	1.58(9)	−310(5)	5.611(3)

Temperatures were measured with a gallium–arsenide diode. The results of these measurements are reported in Table III.

Crystallographic Results

The lattice parameters for the series $Co_{1-x}Ni_xAsS$ ($0 \leqslant x \leqslant 1$) are plotted (Fig. 4) as a function of composition (x). The increase in cell parameter as a function of nickel concentration is linear within experimental error.

This monotonic increase reflects the addition of one electron per substituted nickel atom into the initially empty σ^* antibonding band. There is excellent agreement between the lattice parameters (see Table II) determined for the polycrystalline charge and the corresponding transported single crystal compositions. The cell parameters for end members of the solid solution series are in good agreement with the values reported by previous workers (10, 11).

The X-ray tracings indicated that the preparations were single phase. The sharpness of the peaks and the clear separation of the K_α doublet at higher angles are characteristic of homogenous, well-crystallized materials. A significant result is the appearance and progressive increase in relative intensities of the (110) and (310) cubic reflections at high nickel concentrations ($x \geqslant 0.8$). These reflections are forbidden by the pyrite $Pa3$ space group ($hk0$ possible only when $h = 2n$) and may be indicative of anion ordering.

Intensity data collected for NiAsS samples were used to refine five parameters: anion positions [2], cation position [1], isotropic unit cell temperature factor [1], and variable anion occupancy factor (order–disorder) [1]. The calculations were performed on the basis of a cubic ullmanite structure, space group $P2_13$, Fig. 2. The structure refinement of a mineral sample of NiAsS by Bayliss and Stephenson (10) was determined based on the assumption that the structure was completely ordered. However, in the present study, the degree of anion order was allowed to vary in order to optimize the correlation between observed and calculated data. For this model the best correlation was obtained with 88 % of the anions ordered (i.e., any ordering in the

TABLE III

ELECTRICAL PROPERTIES FOR THE $Co_{1-x}Ni_xAsS$ COMPOUNDS

$Co_{1-x}Ni_xAsS$ Single crystal samples	Carrier type	$\rho(\Omega - cm)$	$R_H(cm^3/C)$	$E_g(eV)$	n(carriers/mole)	$\mu(cm^2/V sec)$
$x = 0.0$	n	1.49×10^{-1}	1.17×10^{-2}	< 0.10		
0.05	n	4.89×10^{-3}	4.75×10^{-3}	—	3.43×10^{22}	9.7×10^{-1}
0.1	n	3.37×10^{-3}	3.30×10^{-3}	—	4.95×10^{22}	9.8×10^{-1}

Cubic $P2_13$				
h	k	l	I_{obs}	I_{calc}
110			11.40	11.41
111			5.96	4.17
200			63.70	56.60
210, 120			100.00	100.00
211			71.10	74.47
220			24.20	28.46
221			0.91	1.06
310, 130			3.23	2.87
311			77.70	76.58
222			10.80	14.15
320, 230			27.30	27.37
321, 123			35.40	35.67
400			3.93	2.81
322, 410, 140			1.02	1.02
411, 330			3.02	3.01
331			2.43	2.46
420, 240			4.65	5.66
421, 124			16.20	15.23

Arsenic position	0.610(5)
Sulfur position	0.381(5)
Nickel position	1.006(5)
Occupancy factor[a]	0.913(5)

[a] To calculate the degree of anion ordering = [(occupancy factor) − (occupancy factor for complete anion disorder (0.5))]/0.5.

anion layer would be an ordered arrangement of As–S alternating pairs along the four [111] directions). Table IV shows the observed and calculated intensities for each reflection. The final values of the variable parameters are listed at the bottom of Table IV. The reliability factor R, which indicates the degree of correlation between the calculated and observed intensities, was 0.054. In pyrite type materials, the 200 and 400 planes are parallel to the {100} cleavage which may lead to preferred orientation of these planes even after extensive grinding. An improved R value of 0.048 resulted upon elimination of the 200 and 400 reflections from the data set.

Electrical and Magnetic Results and Discussion

Electrical resistivity and Hall data (Table III) for single crystals of $Co_{1-x}Ni_xAsS$ ($x = 0.0$, 0.05, 0.10), were collected over the temperature range 77–325°K. CoAsS was found to be semiconducting (9) with a room temperature (296°K) resistivity of $1.49 \cdot 10^{-1}$ Ω cm. The temperature dependence of the resistivity for CoAsS indicated a small energy gap ($E_g \approx 0.05$ eV) which may be indicative of the extrinsic nature of the material. The substitution of a small amount ($x = 0.05$) of nickel for cobalt changed the electrical properties from semiconducting to metallic. The resistivity measurements on the nickel substituted samples exhibited temperature-independent behavior where the resistivity for $Co_{0.95}Ni_{0.05}AsS$ was $5 \cdot 10^{-3}$ Ω cm at 300°K. The Hall-effect measurements also showed temperature-independent behavior and that the charge carriers were electrons; the number of carriers was proportional to the nickel concentration. These results are consistent with the magnetic and crystallographic properties and can be understood on the basis of an introduction of electrons into the σ^* band as Ni is substituted into CoAsS.

Susceptibility data were obtained over the temperature range 77–300°K. The results of the susceptibility measurements are given in Table II. CoAsS showed weak, temperature independent susceptibility ($\chi_M \approx 10 \cdot 10^{-6}$ cgs/mole) characteristic of a diamagnetic material. All other compositions ($0 < x \leqslant 1.0$) exhibited temperature-dependent paramagnetic susceptibility (Figs. 3a and 3b).

As can be seen in Table II, the P_{eff}/Ni for $Co_{1-x}Ni_xAsS$ ($0 < x < 1$) are consistent with the theoretical spin-only value (1.71 μ_B) for low spin Ni (d^7) in an octahedral environment. The Weiss constant θ_p decreased over the compositional range (Fig. 5) from −45(2)°K for $Co_{0.95}Ni_{0.05}AsS$ to −1367(29)°K for $Co_{0.1}Ni_{0.9}AsS$. The rate of decrease of θ_p vs composition x was greater at higher nickel compositions ($x > 0.3$). Corresponding with this decrease of θ_p, the inverse susceptibility curves (Figs. 3a and 3b) show a progressively smaller temperature-dependent behavior as the Ni content is increased. This decrease in the temperature dependence of the inverse
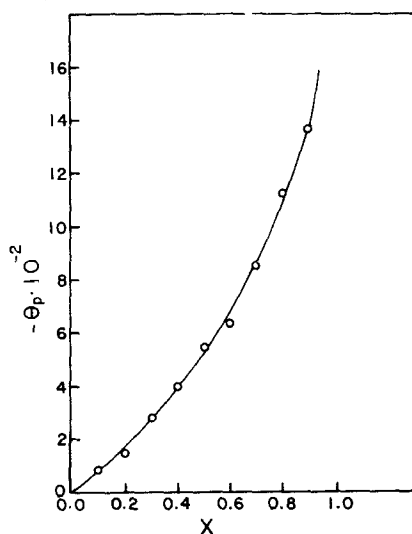
FIG. 5. Weiss constants θ_p vs composition x for $Co_{1-x}Ni_xAsS$ $0 < x < 1$.

susceptibility as well as the change in electrical properties indicates a trend towards Pauli paramagnetic behavior as the nickel content increases.

The ferromagnetic character of the $CoAs_x$-S_{2-x} compositions has been attributed to the correlation of electrons in a narrow σ^* band (4). For compositions of $Co_{1-x}Ni_xAsS$ isoelectronic with $CoAs_{1-x}S_{1+x}$ no evidence of ferromagnetic interactions was found. Goodenough (8) points out that a large σ^* band width precludes the possibility of spontaneous magnetism. He also pointed out that a decreasing energy difference between the σ bonding cation d orbitals and the anion-hybrid orbitals would increase the covalent mixing and result in a broadening of the σ^* antibonding band. The d-orbitals at a nickel atom are more stable than those at a cobalt atom since nickel has the larger effective nuclear charge. This fact has two consequences: (1) the occupied states at the bottom of the σ^* band are primarily associated with the nickel atoms and (2) stronger covalent mixing occurs at the nickel atoms rather than at the cobalt atoms which is consistent with a σ^*-band at the nickel–atom array that is too broad to sustain spontaneous magnetism and that has a band width that increases with nickel concentration x. However, the retention of exchange enhancement by weak correlations and the low electron mobility indicate a narrow σ^* band, which is consistent with spontaneous ferromagnetism in CoS_2.

Acknowledgment

References

1. S. R. BUTLER AND R. J. BOUCHARD, *J. Cryst. Growth* 10, 163 (1971).
2. S. FURUSETH, A. KJEKSHUS, AND A. F. ANDRESEN, *Acta Chem. Scand.* 23, 2325 (1969).
3. K. ADACHI, K. SATO, AND M. TAKEDA, *J. Phys. Soc. Japan* 26, 631 (1969).
4. J. MIKKELSEN AND A. WOLD, *J. Solid State Chem.* 3, 39 (1971).
5. H. S. JARRETT, W. H. CLOUD, R. J. BOUCHARD, S. R. BUTLER, G. G. FREDERICK, AND J. L. GILLSON, *Phys. Rev. Letters* 21, 617 (1968).
6. V. JOHNSON AND A. WOLD, *J. Solid State Chem.* 2, 209 (1970).
7. T. A. BITHER, R. J. BOUCHARD, W. H. CLOUD, P. C. DONOHUE, AND W. J. SIEMONS, *Inorg. Chem.* 7, 2208 (1968).
8. J. B. GOODENOUGH, *J. Solid State Chem.* 3, 26 (1971).
9. H. NAHIGIAN, J. STEGER, H. McKINZIE, R. J. ARNOTT AND A. WOLD, unpublished.
10. P. BAYLISS AND N. C. STEPHENSON, *Mineral. Mag.* 36, 38 (1967).
11. D. D. KLEMM, *Neves Jahrb. Mineral* 103, 205 (1965).
12. D. T. CROMER AND J. T. WABER, *Acta Cryst.* 18, 104 (1965).
13. D. T. CROMER, *Acta Cryst.* 18, 17 (1965).
14. R. ADAMS, Ph.D. Thesis, Brown University, 1973.
15. VOGEL, *Quant. Inorg. Anal.*, p. 418.
16. HILLEBRAND AND LUNDELL, *Applied Inorg.*, p. 315.
17. B. MORRIS AND A. WOLD, *Rev. Sci. Instrum.*, 39, 1937 (1968).
18. B. W. FIGGIS AND R. S. NYHOLM, *J. Chem. Soc.*, 4190 (1958).
19. P. W. SELWOOD, *Magnetochemistry*, Interscience Publishers, New York (1956).
20. L. J. VAN DER PAUW, *Philips Res. Repts.* 13, 1 (1958).